Quick Quantum Steering: Overcoming Loss and Noise with Qudits

Srivastav, Vatshal; Valencia, Natalia Herrera; McCutcheon, Will; Leedumrongwatthanakun, Saroch; Designolle, Sébastien Karl Gérard; Uola, Roope Kristian; Brunner, Nicolas; Malik, Mehul

How to cite

SRIVASTAV, Vatshal et al. Quick Quantum Steering: Overcoming Loss and Noise with Qudits. In: Physical review. X, 2022, vol. 12, n° 4, p. 041023. doi: 10.1103/PhysRevX.12.041023

This publication URL: https://archive-ouverte.unige.ch/unige:165557
Publication DOI: 10.1103/PhysRevX.12.041023

Featured in Physics

Quick Quantum Steering: Overcoming Loss and Noise with Qudits

Vatshal Srivastav,[1,*] Natalia Herrera Valencia,[1] Will McCutcheon,[1] Saroch Leedumrongwatthanakun,[1] Sébastien Designolle,[2] Roope Uola,[2] Nicolas Brunner,[2] and Mehul Malik[1,†]

[1]*Institute of Photonics and Quantum Sciences, Heriot-Watt University, Edinburgh EH14 4AS, United Kingdom*

[2]*Department of Applied Physics, University of Geneva, 1211 Geneva, Switzerland*

(Received 26 April 2022; revised 29 September 2022; accepted 21 October 2022; published 30 November 2022)

A primary requirement for a robust and unconditionally secure quantum network is the establishment of quantum nonlocal correlations over a realistic channel. While loophole-free tests of Bell nonlocality allow for entanglement certification in such a device-independent setting, they are extremely sensitive to loss and noise, which naturally arise in any practical communication scenario. Quantum steering relaxes the strict technological constraints of Bell nonlocality by reframing it in an asymmetric manner, with a trusted party only on one side. However, tests of quantum steering still require either extremely high-quality entanglement or very low loss. Here we introduce a test of quantum steering that harnesses the advantages of high-dimensional entanglement to be simultaneously noise robust and loss tolerant. Despite being constructed for qudits, our steering test is designed for single-detector measurements and is able to close the fair-sampling loophole in a time-efficient manner. We showcase the improvements over qubit-based systems by experimentally demonstrating quantum steering in up to 53 dimensions, free of the fair-sampling loophole, through simultaneous loss and noise conditions corresponding to 14.2-dB loss equivalent to 79 km of telecommunication fiber, and 36% of white noise. We go on to show how the use of high dimensions counterintuitively leads to a dramatic reduction in total measurement time, enabling a quantum steering violation almost 2 orders of magnitude faster obtained by simply doubling the Hilbert space dimension. Our work conclusively demonstrates the significant resource advantages that high-dimensional entanglement provides for quantum steering in terms of loss, noise, and measurement time, and opens the door toward practical quantum networks with the ultimate form of security.

DOI: 10.1103/PhysRevX.12.041023

Subject Areas: Photonics, Quantum Physics
Quantum Information

I. INTRODUCTION

In today's digital landscape riddled with threats such as cyberattacks and information leaks, the advent of secure quantum communication has strongly impacted modern technological progress. Intense research advances have been carried out in the past two decades to achieve a secure and robust implementation of quantum communication between two distant parties [1–5]. The ultimate form of security is provided in the scenario when the two parties, Alice and Bob, can verify entanglement between them in a device-independent (DI) manner [6], i.e., without requiring any trust in their devices or the channels themselves. A requirement for this form of entanglement distribution is a test of quantum nonlocality, such as the loophole-free violation of a Bell inequality, which has been demonstrated over short-distance scales of up to a kilometer [7–9]. However, inevitable loss due to propagation and environmental noise restrict the maximum distance over which entanglement can be certified in a DI manner, making such protocols vulnerable to attacks associated with the fair-sampling loophole (where an eavesdropper could exploit an unjustified fair-sampling assumption) [10,11]. In other words, we must associate our inability to measure every photon that was created with the actions of a malicious eavesdropper "listening in" on the quantum conversation. Closing the fair-sampling loophole is technologically demanding, normally requiring extremely high overall system detection efficiencies, which naturally imposes practical limitations over realistic long-distance channels.

Quantum steering is an alternative scenario that relaxes the rigid technical requirements of device-independent entanglement certification. Here, one can assume that a trusted measurement device exists only on one side [12–14]. In this asymmetric one-sided device-independent (1SDI) setting, entanglement is certified when the untrusted

*vs54@hw.ac.uk
†m.malik@hw.ac.uk

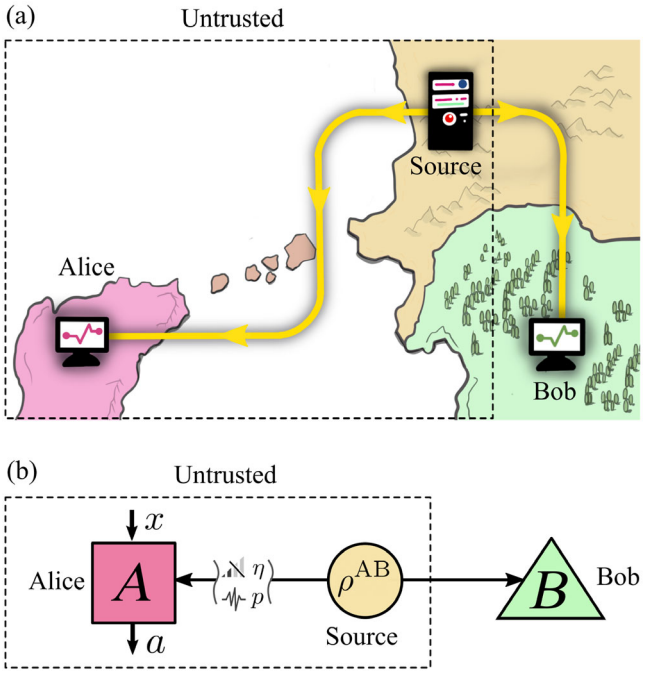

FIG. 1. 1SDI entanglement distribution scenario. The illustration in (a) depicts an example of a fiber-based 1SDI quantum network between two distant stations, Alice and Bob. A source distributes entangled photon pairs to Alice and Bob via optical fiber links. In the 1SDI scenario, the source, Alice's base station, and the fiber link between them are untrusted, for example, due to their geographic location or compromised devices. On the other hand, Bob's station is trusted, and hence, imperfections on his side are ignored. A suitable strategy to certify entanglement in this scenario is given by quantum steering (b), where a bipartite state ρ^{AB} is shared between Alice and Bob. Alice's measurements and the channel between her and the source are affected by loss (η) and noise (p) and considered to be untrusted. By performing local measurements x with outcomes a, Alice conditions the shared state ρ^{AB} to an assemblage $\sigma_{a|x}$ at Bob. Bob can perform suitable measurements on his shared state and check if the state is steerable (thus, entangled) by violating a steering inequality.

party (say, Alice) is able to condition or "steer" the state of the trusted party (Bob) through her local measurements. Note that the fair-sampling loophole is a threat only on Alice's side due to her untrusted measurement apparatus, as well as any loss or noise introduced in the untrusted channel. Since Bob's measurement devices are trusted, he is exempt from the loophole. Figure 1(a) illustrates an example of such a scenario, where Alice and the entanglement source are located in different (untrusted) geographic locations and are connected by an inaccessible (untrusted) undersea fiber-optic channel.

The experimental detection of steering is conveniently achieved via the violation of so-called steering inequalities [15,16]. Experimental violations of such inequalities using qubit entanglement with the fair-sampling loophole closed were reported recently [17–19]. By increasing the number of measurement settings used by both parties, the threshold heralding efficiency required to demonstrate Einstein-Podolsky-Rosen (EPR) steering with qubit entanglement can be lowered arbitrarily in the limit of infinitely many measurement settings. However, this is only possible if Alice and Bob share a high-quality qubit-entangled state, with higher loss requiring increasingly higher-state qualities [18]. In addition to loss, any realistic quantum channel will be prone to sources of noise such as dark and background counts, copropagating classical signals, and imperfect measurement devices. Furthermore, performing a large number of measurements can be impractical, leading to extremely long measurement times in an already lossy scenario [18,20].

It has been established that high-dimensional entanglement can overcome several limitations of qubit-entangled systems [21,22]. Such entangled "qudits" can exhibit stronger correlations than qubit entanglement [23,24] and can tolerate lower heralding efficiency thresholds for tests of nonlocality [25]. Qudits also offer advantages in quantum key distribution [26–28], leading to higher key rates and robustness to noise [29–33]. Notably, the large dimensionality of photonic platforms has enabled entanglement distribution with greater noise resistance [34,35] and higher information encoding capacities [36–40] than qubits. In the realm of quantum steering, the use of qudits has enabled demonstrations of genuine high-dimensional steering as well as increased noise robustness [41,42]. However, these prior demonstrations do not address the critical issue of loss and reconstruct multioutcome measurements via multiple single-outcome measurements, opening them up to the fair-sampling loophole. While the noise robustness offered by high-dimensional entanglement makes it a strong contender for the realization of device-independent quantum-communication protocols [6,43], many practical considerations have hindered its adoption—general multioutcome measurements of high-dimensional quantum states of light are notoriously difficult to realize, e.g., requiring arrays of cascaded, unbalanced interferometers [44] or complex spatial-mode-transformation devices [45,46]. In addition, they are prone to impractically long measurement times and suffer from loss and noise due to the lack of ideal multioutcome detectors.

Here, we overcome many of the challenges associated with high-dimensional photonic systems through simultaneous advances in theory and experiment, allowing us to demonstrate quantum steering with the fair-sampling loophole closed under extreme conditions of loss and noise. First, we formalize a set of linear steering inequalities requiring only a single detector at each party, unlike standard multioutcome measurements that require d detectors for measuring qudits. These inequalities are especially formalized for high dimensions by binarizing projective measurements onto mutually unbiased bases (MUBs) [47] and exhibit the same loss tolerance and noise robustness as

their counterparts designed for multioutcome detectors [48]. In contrast, however, these inequalities provide the strong advantages of needing significantly fewer technological resources and being free from strong assumptions on detector noise, such as background or accidental count subtraction. We violate these steering inequalities experimentally with photon pairs entangled in their discrete transverse position momentum, in the presence of noise and at a record-low heralding efficiency of 0.038 ± 0.001 (approximately 14.2 dB), which is equivalent to the optical loss of a 79-km-long telecommunications fiber [49].

Despite the number of single-outcome measurements scaling with dimension $O(d^2)$, we show that the total measurement time in large d can be reduced considerably thanks to the high statistical significance of a violation in high dimensions for a fixed number of counts. We experimentally verify this by comparing the violations at two different dimensions ($d = 23, 41$) taken at two different acquisition times under a fixed channel loss (approximately 12.1 dB). As a result, we are able to dramatically reduce the total measurement time from 2.53 h for $d = 23$, to 2.5 min for $d = 41$. In both dimensions, we violate the steering inequality by 10 standard deviations. Below, we elaborate on the theoretical formulation of our binarized linear steering inequality, followed by a detailed discussion of the experimental implementation and results.

II. THEORY

In quantum steering, the untrusted party Alice conditions the shared bipartite state ρ^{AB} through her measurement operators $\{A_{a|x}\}$, where x denotes her choice of measurement and a her outcome. By doing so, she creates the conditional (non-normalized) states $\sigma_{a|x} = \mathrm{tr}_A[(A_{a|x} \otimes \mathbb{1}_B)\rho^{\mathrm{AB}}]$, also known as an assemblage. Since the trusted party Bob has access to the assemblage, he can check if $\sigma_{a|x}$ can be produced without the use of entanglement via a so-called local hidden state (LHS) model [12]. A steering inequality [15,16] allows Bob to detect assemblages that do not follow any LHS model and thus demonstrate steering. Formally, it consists of a set of (unnormalized) measurements $\{F_{a|x}\}$ on Bob's side and a value β^{LHS} such that, for all unsteerable assemblages we have that

$$\beta \equiv \sum_{a,x} \mathrm{tr}(F_{a|x}\sigma_{a|x}) \leq \beta^{\mathrm{LHS}}, \tag{1}$$

where β^{LHS} is the maximum value of the functional β for any unsteerable, i.e., LHS assemblage. When using entanglement and appropriate measurements, higher functional values β_Q can be obtained. Hence, steering is demonstrated whenever the above inequality in Eq. (1) is violated, that is, when $\beta_Q > \beta^{\mathrm{LHS}}$.

Here, we formalize a set of linear steering inequalities designed especially for single-outcome projective measurements, which are particularly suitable for single-photon detection systems that are widely implemented on photonic platforms [50,51]. First, we begin with a steering inequality in which Alice and Bob measure d-outcome projective measurements in a given d-dimensional MUB, constructions of which are known to exist for prime and prime power dimensions [47]. Alice (Bob) measures $A_{a|x}$ ($A^T_{a|x}$) with an outcome $a = 0, \ldots, d-1$ in a basis given by $x = 0, \ldots, m$ with $m \leq d$; see Eq. (B1). We then binarize these measurements such that Alice's measurements become

$$\tilde{A}_{\tilde{a}|\tilde{x}}(\eta) = \begin{cases} \eta A_{a|x} & \text{if } \tilde{a} = 1, \\ \mathbb{1} - \eta A_{a|x} & \text{if } \tilde{a} = 0, \end{cases} \tag{2}$$

where η is the one-sided heralding efficiency at Alice. The one-sided heralding efficiency is defined as the probability that detecting a photon at the trusted party (Bob) heralds the presence of a photon at the untrusted party (Alice). Note that the binarized measurements $\tilde{A}_{\tilde{a}|\tilde{x}}$ are labeled by new indices $\tilde{a} = 0, 1$ corresponding, respectively, to a no-click or click event at the detector and $\tilde{x} = (a, x)$, reflecting the new set of measurement settings that includes every projector from each basis. Bob's measurements, which are used to evaluate the steering inequality, are defined in a similar fashion

$$\tilde{F}_{\tilde{a}|\tilde{x}} = \begin{cases} A^T_{a|x} & \text{if } \tilde{a} = 1, \\ c(\mathbb{1} - A^T_{a|x}) & \text{if } \tilde{a} = 0, \end{cases} \tag{3}$$

where $c = 1/(\sqrt{d} - 1)$ is a constant chosen to facilitate the derivation of a closed-form expression for an upper bound $\tilde{\beta}$ on the corresponding LHS bound given by $\tilde{\beta}^{\mathrm{LHS}} \leq 1 + m(\sqrt{d} + 1) \equiv \tilde{\beta}$; see Eq. (A8) in Appendix A. Therefore, obtaining a value of the steering inequality larger than $\tilde{\beta}$ demonstrates steering.

Second, in order to study the effects of noise suffered by the shared state ρ^{AB}, one can consider the isotropic state that includes a fraction of added white noise, specifically, $\rho^{\mathrm{AB}}(p) \equiv p|\phi_d\rangle\langle\phi_d| + (1-p)\mathbb{1}_{d^2}/d^2$, where $|\phi_d\rangle \equiv \sum_{i=0}^{d-1} |ii\rangle/\sqrt{d}$ is the maximally entangled state in dimension d, and $p \in [0, 1]$ is the noise mixing parameter. Finally, we use Eq. (1) to evaluate the functional β^Q in terms of one-sided heralding efficiency η and mixing parameter p; see Eq. (A9). To check the violation of the steering inequality, we calculate the difference between $\beta^Q(\eta, p)$ and $\tilde{\beta}$ (upper bound on $\tilde{\beta}^{\mathrm{LHS}}$), which is given as

$$\Delta\beta = \eta m\left(p - \frac{1-p}{\sqrt{d}}\right) - 1. \tag{4}$$

The condition $\Delta\beta > 0$ must be satisfied in order to demonstrate steering, which also leads to a critical value η^{cr} for the one-sided heralding efficiency η. The critical heralding efficiency η^{cr} generally depends on the noise

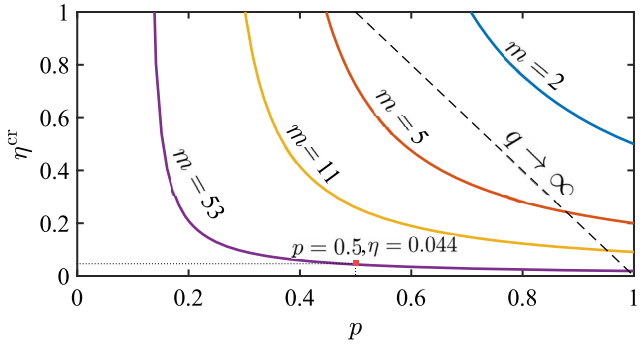

FIG. 2. Noise robustness and loss tolerance. Dependence of the critical heralding efficiency η^{cr} for Alice with respect to the noise parameter p in the bipartite shared state $\rho^{AB}(p)$ when using $m = d$ MUB measurement settings to demonstrate EPR steering in dimension d. By increasing the number of measurement settings m (or increasing the dimensions d), the critical efficiency η^{cr} decreases substantially, even at significant noise levels ($p < 1$). For example, with $m = 53$ MUB settings, one can tolerate a heralding efficiency as low as $\eta = 0.044$ and a noise parameter $p = 0.5$ (equal mixture of maximally entangled state and white noise). In contrast, demonstrating steering with qubit entanglement ($d = 2$) requires significantly higher heralding efficiencies η_{cr} and a noise parameter $p > 0.5$ in the impractical limit of infinite measurement settings ($q \to \infty$, dashed line) [18]. Thus, high-dimensional entanglement enables us to access regimes of noise and loss that are inaccessible by qubit entanglement, even in the best-case scenario.

parameter p, the number of MUB measurement settings m, and the dimension of the Hilbert space d [see Eq. (A10)]. In the noise-free case ($p = 1$), the critical one-sided heralding efficiency can be reduced to $\eta^{cr} = 1/m$, the lowest possible value [52], which can also be obtained with qubits [18]. However, any experiment features noise, i.e., with a mixing parameter $p < 1$, originating from various technical imperfections ranging from detector dark counts or multipair emission to misalignments in the system [35]. As the amount of noise increases, it can be shown that the value of η^{cr} required to demonstrate steering increases; see Eq. (A10). For qubits ($d = 2$), the required critical efficiency η^{cr} to demonstrate steering reaches unity when the noise parameter $p \sim 0.71$ for $m = 2$ measurements, while steering is impossible for $p \leq 1/2$ [12,53].

In contrast, Fig. 2 shows that by increasing the number of MUB measurement settings m, which is only possible in the qudit regime ($d > 2$), one can still demonstrate steering in the presence of substantial loss and noise in the channel as compared to qubit-based systems. For example, using 53 MUB settings, one can tolerate a heralding efficiency as low as $\eta = 0.044$ and a noise parameter of $p = 0.5$. This enables one to find the perfect trade-off between loss in the channel and noise in the system. Additionally, with our binarized steering inequalities, projective measurements with only two outcomes (photon detected or not detected) not only show the same loss tolerance and noise robustness as their multioutcome counterparts for steering [48], but are also more feasible to implement experimentally with two single-click photon detectors that are typically available in every photonics laboratory.

A key practical requirement for demonstrating these methods is the acquisition of sufficient data to report results within a desired confidence interval. By considering the variance of our estimator for β^Q, as well as the corresponding expected violation $\Delta\beta$, we can determine the required measurement time. To explore this dependence, we provide an explicit derivation of the required measurement time as a function of the dimension in Appendix C.

III. EXPERIMENT

To experimentally demonstrate noise-robust EPR steering with the fair-sampling loophole closed, we use pairs of photons entangled in their discrete transverse position-momentum degree of freedom, also known as pixel entanglement [54,55]. As shown in Fig. 3(a), two spatially entangled photons at 1550 nm are generated in a 5-mm periodically poled pottasium titanyl phosphate (ppKTP) crystal through the process of type-II spontaneous parametric down-conversion using a Ti:sapphire femtosecond pulsed laser with 500-mW average power. After being separated by a polarizing beam splitter, each photon from the entangled pair is directed to the two parties Alice and Bob, who can perform local projective measurements by using a spatial light modulator (SLM) to display tailored phase-only holograms. These holograms allow the measurement of a general superposition of spatial modes, i.e., a state from any MUB. Only photons carrying the correct states are efficiently coupled into single-mode fibers, which lead to two superconducting nanowire detectors connected to a coincidence logic. This measurement system allows Alice and Bob to perform the local measurements in Eqs. (2) and (3) and evaluate the elements of the functional in Eq. (1) in terms of the normalized coincidence counts between them and of the normalized exclusive single counts measured by Bob; see Eq. (B6) in Appendix B.

To close the fair-sampling loophole on Alice's side, her measurement basis is designed using hexagonal pixels of equal size with zero spacing between them. This enables Alice to maximize the detection efficiency of her SLM and channel. Bob's measurement basis design is informed by prior knowledge of the two-photon joint-transverse-momentum amplitude (JTMA) [54], which allows him to tailor his pixel mask in order to optimize the resultant one-sided heralding efficiency in the experiment η^{exp} (see Appendix B). The choice of the phase-only pixel basis gives the added advantage that projective measurements in mutually unbiased bases provide the highest possible SLM heralding efficiency, since they do not require any amplitude modulation in their holograms [56]. Furthermore, the two-photon state encoded in the pixel basis can be designed

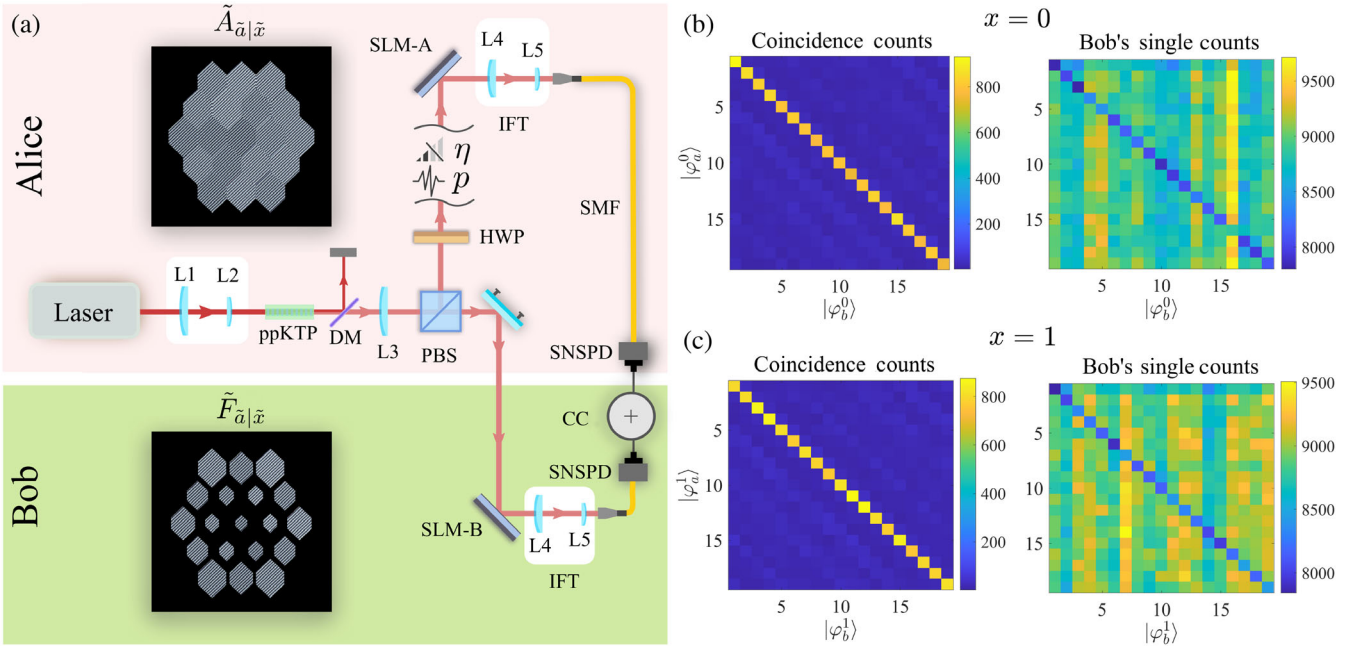

FIG. 3. Experimental setup. (a) A Ti:sapphire pulsed laser at 775 nm is used to pump a nonlinear ppKTP crystal to generate a pair of photons entangled in their transverse position momentum via type-II spontaneous parametric down-conversion. The pump photons are filtered by a dichroic mirror (DM) and the down-converted photons are separated with a polarizing beam splitter (PBS). One photon from the entangled photon pair is sent to the untrusted party, Alice, who generates holograms on a spatial light modulator (SLM-A) to perform the projective measurements $\tilde{A}_{\tilde{a}|\tilde{x}}$; see Eq. (2). Bob receives the other photon along with the outcome $\tilde{a}$ from Alice, forming the assemblage $\sigma_{\tilde{a}|\tilde{x}}$. He then performs the projective measurements $\tilde{F}_{\tilde{a}|\tilde{x}}$ [Eq. (3)] according to the steering inequality defined in Eq. (1). Each of the photons in the selected mode are collected by a combination of telescope lenses (L4 and L5) into single-mode fibers (SMFs) and are detected by superconducting nanowire detectors (SNSPDs). Coincident detection events corresponding to joint two-photon measurements are recorded by a coincidence counting logic (CC) with a coincidence window of 0.2 ns. (b),(c) Experimental data showing coincidence counts between Alice and Bob and exclusive single counts measured on Bob's side in dimension $d = 19$ using MUB measurement settings $x = 0, 1$.

to be close to a maximally entangled state in dimension d owing to the knowledge of the JTMA of the generated two-photon state, which maximizes its entanglement of formation [54,55]. In our experiment, we utilize the crosstalk between individual pixels as a reliable measure of the system noise parameter [p^{exp}; see Eq. (B10)]. This measure is valid because the amount of crosstalk between discrete spatial modes does not change substantially across the MUBs and thus behaves isotropically (see Appendix B for more details).

IV. RESULTS

In our experiment, we demonstrate detection-loophole-free steering in up to dimension $d = 53$ by performing binarized projective measurements in a number of MUBs ranging from $m_{\text{min}} = 12$ to $m_{\text{max}} = 53$. We exclude the computational (hex-pixel) basis in every dimension due to its much higher loss. The system noise parameter (p^{exp}) ranges from $p^{\text{exp}} = 0.823$ to 0.625 and is shown in Fig. 4(a) for every dimension. In dimensions $d \geq 17$, we introduce additional loss on Alice's channel by decreasing the diffraction efficiency of SLM-A and thus reducing the one-sided heralding efficiency $\eta^{\text{exp}} \to \eta^{\text{cr}}(m = d)$ until the state becomes just unsteerable [Fig. 4(b)]. For these reduced η^{exp}, we are able to demonstrate steering with $m = d$ MUB measurement settings. Using $m = 53$ MUB settings, for example, we are able to tolerate a record-low one-sided heralding efficiency of $\eta^{\text{exp}} = 0.038 \pm 0.001$, and violate our steering inequality by more than 8 standard deviations. Note that this violation is obtained under noise conditions corresponding to $p^{\text{exp}} = 0.641$. With lower noise, the one-sided heralding efficiency can be lowered further.

We use our result in $d = 41$ to highlight the tolerance to loss enabled by the use of high dimensions. Figure 4(c) shows the critical one-sided heralding efficiency $\eta^{\text{cr}}(m)$ required to demonstrate steering in $d = 41$ using m measurement settings, as a function of noise parameter p. As m is increased, the critical efficiency at a given noise level can be significantly reduced. For example, at the fixed noise level $p^{\text{exp}} = 0.625$, we are able to demonstrate steering with a one-sided heralding efficiency of $\eta^{\text{exp}} = 0.175$ using $m = 11$ measurement settings. Note that this is possible as long as η^{exp} satisfies $\eta^{\text{exp}} > \eta^{\text{cr}}(m)$. As we increase the number of measurement settings up to $m = 41$, Alice's channel efficiency can be further reduced by a

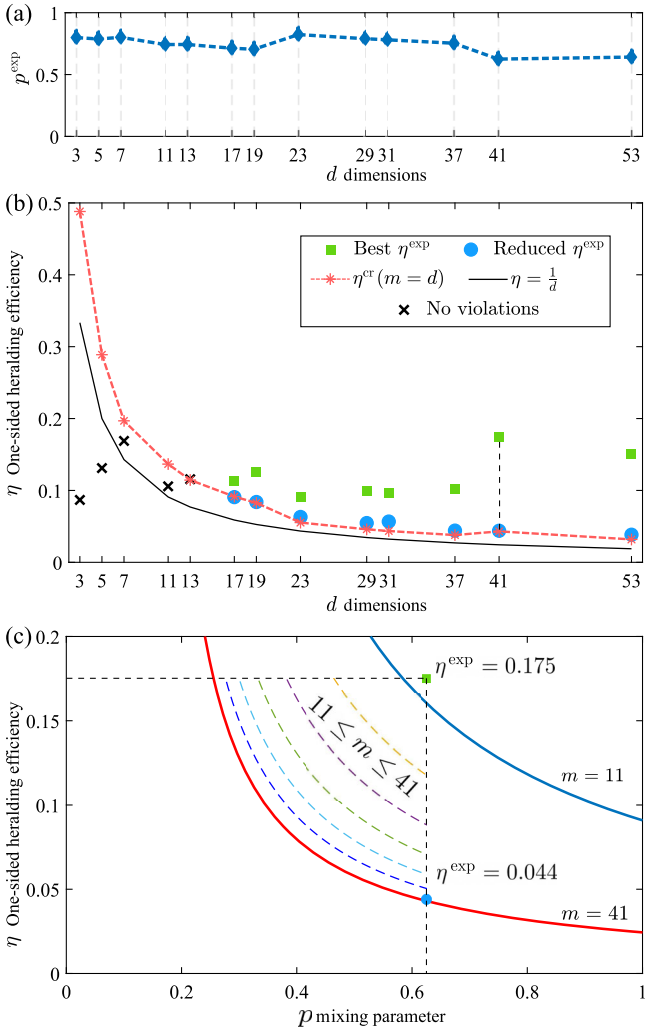

FIG. 4. Experimental results. (a) The experimental noise mixing parameter $p^{\exp}$ as a function of the state dimension d corresponding to a $(1-p)$ fraction of white noise present in the state. (b) The critical one-sided heralding efficiency required to demonstrate steering decreases as a function of d, as shown for the noise-free case (η with $p=1$, solid black curve) and nonideal state quality (η^{cr} with $p^{\exp}<1$, dashed red curve). In dimensions $3\le d<17$ (black crosses), our experimental one-sided heralding efficiency is under the critical value $[\eta^{\exp}<\eta^{\mathrm{cr}}(m=d)]$; thus, the state does not demonstrate steering. In dimensions $d\ge 17$, we are able to demonstrate steering with similarly low heralding efficiencies $\eta^{\exp}$ (green squares) by using $m=d$ MUB settings. The experimental heralding efficiency can be lowered further (blue dots) by adding loss in Alice's channel, allowing us to demonstrate EPR steering in $d=53$ with a record low $\eta^{\exp}=0.038$ and a noise parameter $p^{\exp}=0.641$. (c) To showcase the loss tolerance of our binarized steering inequality, we focus on the case at $d=41$. At $\eta^{\exp}=0.175$, one can demonstrate steering with fewer measurement settings ($m=11$). However, when Alice's channel efficiency is reduced by a factor of 4 to $\eta^{\exp}=0.044$, EPR steering can still be demonstrated by using more measurement settings ($m=41$).

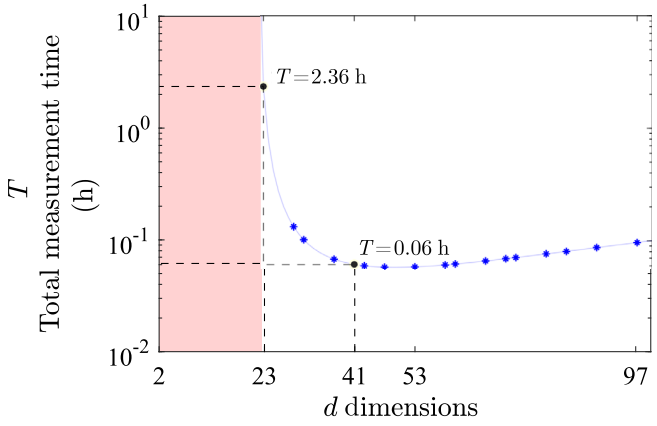

FIG. 5. Dependence of total measurement time (T) on dimension (d). The total measurement time T (on log scale) required to violate the steering inequality by 10 standard deviations can be calculated from Eq. (C7) as a function of the prime dimension d for $m=d$ measurement settings, for a fixed one-sided heralding efficiency $\eta=0.062$ and noise parameter $p=0.775$. The total time taken to obtain a steering violation using $m=23$ measurement settings in dimension $d=23$ is 2 orders of magnitude larger than that with $m=d=41$.

factor of 4 to $\eta^{\exp}=0.044$ and still demonstrate quantum steering. This clearly demonstrates the increased robustness to loss enabled by high dimensions in detection-loophole-free steering violations. In general, the amount of loss and noise tolerated can be optimized by working along the critical one-sided heralding efficiency curves shown in Fig. 4(c) for a given number of measurement settings.

A common problem encountered in experiments with qudits is that the total measurement time (T) increases drastically with the dimension of the Hilbert space, as the total number of single-detector measurements scales as md^2. For our binarized steering inequality, we show that this is indeed not the case when one considers a steering violation within a fixed confidence interval. Consider the example shown in Fig. 5, where for a given amount of noise and loss, a steering violation is obtained only in dimensions $d\ge 23$. As d is increased, the total measurement time T required to violate the steering inequality by 10 standard deviations decreases dramatically till it attains a minimum, and then gradually increases again. This allows us to minimize T over larger dimensions at which the resilience against loss and noise is substantially high and still demonstrate steering in a practical measurement time (see Appendix C for a detailed derivation). We verify this result in our experiment by comparing the experimental data taken at two different dimensions ($d_1=23$, $d_2=41$) using $m=d$ settings, at a fixed one-sided heralding efficiency $\eta^{\exp}=0.062\pm0.006$ and noise parameter $p^{\exp}=0.775$, but with two very different acquisition times

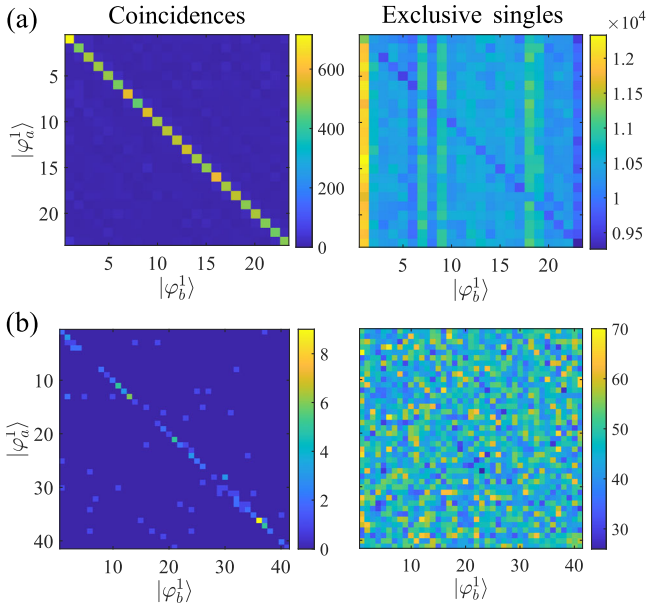

FIG. 6. Time-efficient steering in high dimensions. The coincidence counts between Alice and Bob and exclusive single counts measured by Bob in measurement basis $x = 1$ in dimension (a) $d = 23$ and (b) $d = 41$ at a fixed one-sided heralding efficiency of $\eta^{\text{exp}} \sim 0.062$, detected with two different acquisition times. Interestingly, even though the counts in $d = 41$ are 2 orders of magnitude lower than in $d = 23$, we still violate the steering inequality with 10 standard deviations in both cases.

($t_1^{\text{ac}} = 750$ ms, $t_2^{\text{ac}} = 2.2$ ms) (see Table I). For $d_1 = 23$, the total measured singles counts per acquisition window are around 10^4, while for $d_2 = 41$, counts are lowered over 100 times to about 70. The coincidence counts in $d_2 = 41$ are just a few counts per second, on the order of the crosstalk (see Fig. 6). While these two cases both demonstrate a violation of the steering inequality by 10 standard deviations, $d_2 = 41$ achieves a substantial reduction in the total measurement time ($T_1 = 2.53$ h and $T_2 = 2.53$ min). Note that the response time of the spatial light modulators is excluded from the total measurement time T, as this is a technical limitation that can be addressed by using a fast phase modulation device such as a digital mirror device [57].

V. CONCLUSION AND OUTLOOK

We introduce a set of noise-robust EPR steering inequalities in high dimensions, specially designed for single-outcome detectors, that showcase the same loss tolerance as their multioutcome counterparts. We report the violation of our EPR steering inequality with the fair-sampling loophole closed, with a record-low one-sided heralding efficiency of $\eta = 0.038$ and a noise mixing parameter of $p^{\text{exp}} = 0.641$, which is equivalent to the loss in a 79-km-long telecommunication fiber and 35.9% white noise. We are able to achieve this level of noise and loss tolerance by harnessing spatial entanglement in Hilbert space dimensions up to $d = 53$. The amount of loss and noise that these inequalities can tolerate can be increased substantially by increasing the entanglement dimension d. For instance, in $d = 499$, the maximum tolerable loss to demonstrate steering increases to 27 dB, which is equivalent to the loss in a 135-km-long telecom optical fiber. Similarly, the maximum amount of white noise that can be allowed in the system while violating the steering inequality at unit heralding efficiency reaches 95%. Finally, we demonstrate that the total measurement time required to demonstrate steering can be significantly reduced through the use of high dimensions. For a fixed amount of noise and loss, the total integration time required to violate our steering inequality by 10 standard deviations can be lowered 60 times through a modest increase to the Hilbert space dimension ($d = 23$ to $d = 41$).

TABLE I. Experimental measurement time T required for a steering violation in two different dimensions d.

d	η^{exp}	t^{ac}	T	$\langle S \rangle$
23	0.063 ± 0.001	750 ms	2.53 h	$\sim 10^4$
41	0.062 ± 0.006	2.2 ms	2.53 min	~ 70

Our demonstration of time-efficient quantum steering under realistic environmental conditions holds significant promise for the future development of one-sided device-independent quantum-communication protocols. Any long-distance communication channel, such as one relying on optical fiber or free-space transmission, necessarily includes loss due to light leakage or scattering and noise due to modal dispersion or atmospheric turbulence. The steering inequalities presented here demonstrate a way to overcome these detrimental effects through the use of high-dimensional entanglement. It is important to note that our methods, in particular, our single-detector steering inequality, are not limited to the spatial degree of freedom, but can readily be extended to other photonic properties such as time frequency [58] or path encoding in a photonic integrated circuit [59]. Our methods could also be helpful in the demonstration of quantum memory networks on photonic platforms, which currently require high-efficiency channels for transmission, thus extending the scalability limits of long-range quantum networks [60,61]. Our resource-efficient steering protocol fulfills an important prerequisite for establishing security between malicious servers and clients, and future work toward greater device independence for attacks on detector efficiency, for instance [62], would further progress 1SDI quantum key distribution [63], as well as private quantum computing and related protocols [64]. Above all else, our demonstration of quantum steering under prohibitive conditions of noise and loss shows that the fundamental phenomenon of entanglement can indeed transcend the limits imposed by a realistic environment, when one makes full use of the inherently high-dimensional photonic Hilbert space.

ACKNOWLEDGMENTS

This work is made possible by financial support from the QuantERA ERA-NET Co-fund (FWF Project No. I3773-N36), the UK Engineering and Physical Sciences Research Council (Grant No. EP/P024114/1), and the European Research Council Starting Grant PIQUaNT No. 950402. N. B., S. D., and R. U. acknowledge financial support from the Swiss National Science Foundation (Project No. 192244, Ambizione Grant No. PZ00P2-202179, and NCCR QSIT).

APPENDIX A: DETAILS FOR $\tilde{\beta}$ AND $\beta^{Q}(\eta, p)$

First, we compute an upper bound $\tilde{\beta}$ on the LHS bound $\tilde{\beta}^{\mathrm{LHS}}$ for the Bob's binarized measurements defined in Eq. (3). We begin with the general definition of LHS bound given in Ref. [13]

$$\tilde{\beta}^{\mathrm{LHS}} = \max_{\tilde{\mu}} \left\| \sum_{\tilde{a},\tilde{x}} \tilde{D}_{\tilde{\mu}}(\tilde{a}|\tilde{x}) \tilde{F}_{\tilde{a}|\tilde{x}} \right\|_{\infty}, \tag{A1}$$

which can be rewritten as

$$\tilde{\beta}^{\mathrm{LHS}} = \max_{\tilde{\mu}} \tilde{\beta}^{\mathrm{LHS}}_{\tilde{\mu}}, \quad \text{where } \tilde{\beta}^{\mathrm{LHS}}_{\tilde{\mu}} \equiv \left\| \sum_{\tilde{x}} F_{\tilde{\mu}_{\tilde{x}}|\tilde{x}} \right\|_{\infty}. \tag{A2}$$

For a given deterministic strategy $\tilde{\mu}$, we write $\tilde{x} \in \tilde{\mu}$ for all $\tilde{x} = (a, x)$ such that $\tilde{\mu}_{\tilde{x}} = 1$ and the complement (corresponding to $\tilde{\mu}_{\tilde{x}} = 0$) is $\tilde{x} \notin \tilde{\mu}$. Following this notation, $|\tilde{\mu}|$ is the number of $\tilde{x}$ such that $\tilde{x} \in \tilde{\mu}$. Using the definition of Eq. (3), we get

$$\tilde{\beta}^{\mathrm{LHS}}_{\tilde{\mu}} = \left\| \sum_{\tilde{x}\in\tilde{\mu}} A_{a|x} + c \sum_{\tilde{x}\notin\tilde{\mu}} (\mathbb{1} - A_{a|x}) \right\|_{\infty} \tag{A3}$$

$$= c[m(d-1) - |\tilde{\mu}|] + (1+c) \left\| \sum_{\tilde{x}\in\tilde{\mu}} A_{a|x} \right\|_{\infty}. \tag{A4}$$

The expression in Eq. (A4) is true using the fact that for any positive semidefinite $\alpha\mathbb{1} + B$, where α is real (not necessarily positive) constant and B is positive semidefinite with eigendecomposition $\sum_j \lambda_j |\lambda_j\rangle\langle\lambda_j|$, can be written as

$$\|\alpha\mathbb{1} + B\|_{\infty} = \max_j \lambda_j + \alpha, \tag{A5}$$

since the eigenvalues $\lambda_j + \alpha$ are positive by assumption.

To continue the computation after Eq. (A4), we make use of the bound

$$\left\| \sum_{\tilde{x}\in\tilde{\mu}} A_{a|x} \right\|_{\infty} \leq 1 + \frac{|\tilde{\mu}| - 1}{\sqrt{d}}, \tag{A6}$$

which is similar to results given in Refs. [65–67], though it becomes increasingly loose particularly for $|\tilde{\mu}| > m$. We then get

$$\tilde{\beta}^{\mathrm{LHS}}_{\tilde{\mu}} \leq \frac{(1+c)(\sqrt{d}-1)}{\sqrt{d}} + cm(d-1) + \frac{1 - c(\sqrt{d}-1)}{\sqrt{d}} |\tilde{\mu}|, \tag{A7}$$

so that there is a natural choice of $c = (1/\sqrt{d} - 1)$ that allows us to get an upper bound independent of $\tilde{\mu}$. With this value, we eventually obtain the desired bound

$$\tilde{\beta}^{\mathrm{LHS}} \leq 1 + m(\sqrt{d} + 1) \equiv \tilde{\beta}. \tag{A8}$$

Next, we evaluate the quantum value β^{Q} of the functional in Eq. (1) for binarized measurements of Alice and Bob performed on a shared maximally entangled state influenced by isotropic noise $\rho^{\mathrm{AB}}(p)$ in terms of one-sided heralding efficiency η, mixing parameter p, and we get

$$\beta^{Q}(\eta, p) = m \left\{ \frac{1-p}{d} [\eta + (d-\eta)(\sqrt{d}+1)] + p(\eta + \sqrt{d} + 1) \right\}, \tag{A9}$$

where d is the dimension of the Hilbert space, and m is the number of MUB measurement settings out of $d+1$ MUBs given for prime dimension d [47].

With $\beta^{Q}(\eta, p)$ and $\tilde{\beta}$, we can simply calculate $\Delta\beta$ [see Eq. (4)], from where we can check that to violate the steering inequality, η must be greater than a threshold η^{cr},

$$\eta > \frac{1}{m(p - \frac{1-p}{\sqrt{d}})} \equiv \eta^{\mathrm{cr}}. \tag{A10}$$

For a pure maximally entangled state ($p = 1$), the above threshold reduces to simply $\eta^{\mathrm{cr}} = (1/m)$.

APPENDIX B: EXPERIMENTAL DETAILS

Because of our loose pump focusing on the ppKTP crystal, we have an initial heralding efficiency of approximately 50%. Additional losses are introduced by our measurement apparatus, where spatial light modulators have a diffraction efficiency of approximately 70%, the telescopes and single-mode fibers used to mode match the collection to multiple spatial modes result in a coupling efficiency of approximately 50%, and our superconductor nanowire detectors have an efficiency of approximately 90%. As shown in Ref. [54], Bob's projective measurements can be optimized from the prior information of the JTMA, such that the resultant one-sided heralding efficiency for Alice increases. In our experiment, we employ

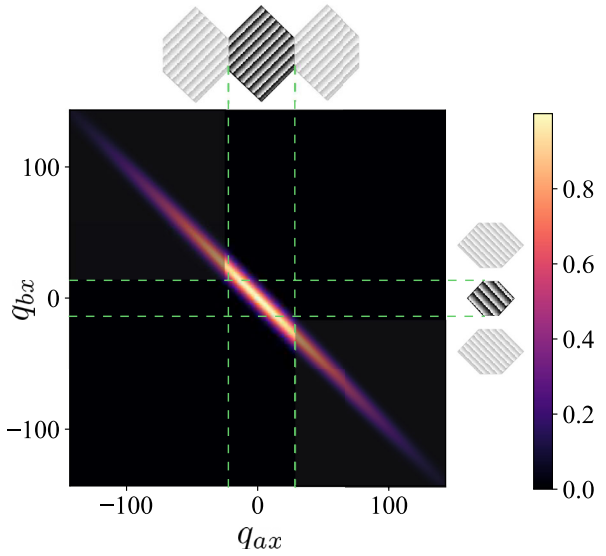

FIG. 7. Optimization of one-sided heralding efficiency. The one-sided heralding efficiency, or the probability that detecting a photon at the trusted party (Bob) heralds the presence of a photon at the untrusted party (Alice), can be optimized from knowledge of the two-photon JTMA [54]. The size of Bob's hex pixels can be set in such a manner that the probability of coincidence counts between Alice and Bob is increased while the probability of single counts at Bob is decreased, effectively increasing the one-sided heralding efficiency η at Alice.

the same optimization to tailor the pixel masks used for Bob's projective measurements, resulting in Bob's pixel sizes being smaller than that of Alice (see Fig. 7). This results in the maximum one-sided heralding efficiency of 17.5% in $d = 41$. Additionally, the spacing between the macropixels in Bob's mask is chosen such that the coincidence counts between different modes (crosstalk) are suppressed [see Fig. 3(a)].

The holograms on SLM on Alice and Bob perform projective MUB measurements $A_{a|x} = |\varphi_a^x\rangle\langle\varphi_a^x|$ on the entangled photons. They are designed according to the prescription given in Ref. [47]

$$|\varphi_a^x\rangle = \frac{1}{\sqrt{d}}\sum_{l=0}^{d-1}\omega^{al+xl^2}|l\rangle, \tag{B1}$$

where $\omega = \exp(2\pi i/d)$ is a dth root of the unity. The first basis is the computational one (individual pixel mode) denoted $\{|l\rangle\}_{l=0}^{d-1}$ and the other d bases are $\{|\varphi_a^x\rangle\}_{a=0}^{d-1}$ labeled by $x = 0, \ldots, d-1$.

To evaluate our steering inequality in the experiment, we use coincidence counts (when both Alice's and Bob's detectors click simultaneously) and Bob's exclusive single counts (when only Bob's detectors click while Alice measures no clicks). For xth basis outcome or projector a and b on Alice and Bob, the coincidence counts (C_{ab}^x) and exclusive single counts on Bob's side (S_{ab}^x) are given as

$$C_{ab}^x := N_x^a \operatorname{tr}[A_{1|ax} \otimes \Pi_{b|x}\rho^{AB}], \tag{B2}$$

$$S_{ab}^x := N_x^a \operatorname{tr}[A_{0|ax} \otimes \Pi_{b|x}\rho^{AB}], \tag{B3}$$

where N_x^a is the total count measured by Bob. Hence, it must satisfy $N_a^x = \sum_b (C_{ab}^x + S_{ab}^x)$.

Bob can then normalize the data by

$$\tilde{C}_{ab}^x := C_{ab}^x / N_a^x, \tag{B4}$$

$$\tilde{S}_{ab}^x := S_{ab}^x / N_a^x \tag{B5}$$

to obtain the steering inequality elements,

$$\operatorname{tr}[\tilde{F}_{\tilde{a}|\tilde{x}}\sigma_{\tilde{a}|\tilde{x}}] = \begin{cases} \tilde{C}_{aa}^x, & \tilde{a} = 1, \\ c\sum\limits_{b\neq a}\tilde{S}_{ab}^x, & \tilde{a} = 0, \end{cases} \tag{B6}$$

and the inequality can be evaluated by

$$\beta^Q = \sum_{a,x}\left(\tilde{C}_{aa}^x + c\sum_{b\neq a}\tilde{S}_{ab}^x\right). \tag{B7}$$

Similarly, we calculate the one-sided heralding efficiency $\eta^{\exp}$ for the xth measurement setting on Alice's channel from

$$\eta^{\exp} = \sum_{a,b}\tilde{C}_{ab}^x. \tag{B8}$$

Note that in our work we perform only $m = d$ MUB measurements excluding the computational basis. The one-sided heralding efficiency $\eta^{\exp}$ for each MUB measurement (not the computational basis) in dimensions d does not vary significantly. To characterize the level of noise in the system, we use the amount of crosstalk v between pixel modes:

$$v = \frac{\sum_a \tilde{C}_{aa}^x}{\sum_{ab}\tilde{C}_{ab}^x}. \tag{B9}$$

This estimate is valid because the v does not change substantially across the MUBs, and thus it behaves isotropically. Formally, the mixing parameter $p^{\exp}$ in the experiment is given as

$$p^{\exp} = \frac{vd-1}{d-1}. \tag{B10}$$

APPENDIX C: MINIMIZING TOTAL MEASUREMENT TIME T

The expectation (mean) number of coincidences and exclusive single counts at Bob's side are

$$\langle C^x_{ab}\rangle = N\eta\left(\frac{p\delta_{ab}}{d}+\frac{1-p}{d^2}\right), \tag{C1}$$

$$\langle S^x_{ab}\rangle = \frac{N}{d} - C^x_{ab}, \tag{C2}$$

where $N = Rt^{\mathrm{ac}}$ is the total number of copies of the state Bob receives during an acquisition window t^{ac} given the underlying single-count rate R detected at Bob's side. In our experiment, we assume that the single-count rates R does not vary significantly for different dimensions. Since the statistics of the raw counts are Poissonian, their variances are $\mathrm{Var}(C^x_{ab}) = \langle C^x_{ab}\rangle$ and $\mathrm{Var}(S^x_{ab}) = \langle S^x_{ab}\rangle$. We can estimate the variance of β^Q by

$$\mathrm{Var}(\beta^Q) = \sum_{xab}\left[\left(\frac{\partial\beta}{\partial C^x_{ab}}\right)^2\mathrm{Var}(C^x_{ab}) + \left(\frac{\partial\beta}{\partial S^x_{ab}}\right)^2\mathrm{Var}(S^x_{ab})\right], \tag{C3}$$

which is inversely proportional to N (and therefore, R and t^{ac}), so we can factor out

$$\mathrm{Var}(\beta^Q) = \frac{f(\eta,p,d,m)}{N}, \tag{C4}$$

where $f(\eta,p,d,m)$ is a function of η, p, d, and m which is independent of N (equivalent to R and t^{ac}). We wish to find the dimension that minimizes the total experiment time $T = t^{\mathrm{ac}}md^2$ while violating the steering inequality by 10 standard deviations. For an expected violation $\Delta\beta$, we require

$$\Delta\beta \geq 10\sqrt{\mathrm{Var}(\beta^Q)}. \tag{C5}$$

From Eqs. (C4) and (C5), we can then solve for N,

$$N \geq 10^2\frac{f(\eta,p,d,m)}{(\Delta\beta)^2}, \tag{C6}$$

which is valid only when $\Delta\beta > 0$. We then evaluate the total measurement time to saturate the bound,

$$T = \frac{Nmd^2}{R} = \frac{md^2 10^2}{R}\frac{f(\eta,p,d,m)}{(\Delta\beta)^2}. \tag{C7}$$

Interestingly, at fixed value of η and p, for $m = d$ measurement settings, the expression $md^2 f(\eta,p,d,m)/(\Delta\beta)^2$ depends nonmonotonically on dimension d. This makes the total measurement time T to reach a minimum at a nontrivial dimension d. At fixed heralding efficiency $\eta = 0.062$, noise level $p = 0.775$, and $m = d$, the expression of T can be simplified and is given as

$$T = \frac{d^2}{R}\frac{[5d^{\frac{5}{2}} - 14d^2 + 100d^{\frac{3}{2}} + 107d - 3\sqrt{d} + 0.19]}{(\sqrt{d}-1)(1+0.01\sqrt{d}-0.05d)^2}. \tag{C8}$$

The plot in Fig. 5 shows the dependence of T with respect to d at rate $R \sim 10^5$.

APPENDIX D: EXTENSION TO GENERAL STEERING INEQUALITIES

A crucial question is whether other families of steering inequalities defined for all dimensions will have the same benefit of decreased measurement times from increased dimensions. While each family of inequalities must be dealt with individually, we can identify the prerequisite. Under weak assumptions, we can show an optimum nontrivial dimension that likely exists where the total measurement time is minimum.

We start by fixing the measure of confidence, i.e., the number of standard deviations σ_n of a steering violation:

$$\frac{\beta^Q - \beta^{\mathrm{LHS}}}{\sqrt{\mathrm{Var}(\beta^Q)_\Gamma}} = \sigma_n. \tag{D1}$$

Here, $\mathrm{Var}(\beta^Q)_\Gamma$ is the variance of the β^Q measured experimentally in a total of Γ trials (corresponding to $\Gamma = Nmd^2$ from Appendix C). The term $\beta^Q - \beta^{\mathrm{LHS}}$ is the amount of violation for the steering inequality. It is important to note that the variance of a maximum likelihood estimator, here $\mathrm{Var}(\beta^Q)_\Gamma$, goes as $1/\Gamma$. Therefore, we can write

$$\mathrm{Var}(\beta^Q)_\Gamma = \frac{1}{\Gamma}\mathrm{Var}(\beta^Q)_{\Gamma=1} \equiv \frac{\mathrm{Var}(\beta^Q)}{\Gamma}. \tag{D2}$$

The number of trials Γ is proportional to the total measurement time T [see Eq. (C7)]. Using Eqs. (D1) and (D2), we can then further simplify

$$T \propto \Gamma = \sigma_n^2\frac{\mathrm{Var}(\beta^Q)}{(\beta^Q - \beta^{\mathrm{LHS}})^2}, \tag{D3}$$

where σ_n is fixed. Note that the above expression is defined only when there is a nonzero violation of a steering inequality, i.e., $\beta^Q - \beta^{\mathrm{LHS}} > 0$. The total measurement time T will decrease with increasing dimension d if

$$\frac{\Delta T}{\Delta d} \propto \frac{1}{\Delta d}\Delta\left(\frac{\mathrm{Var}(\beta^Q)}{(\beta^Q - \beta^{\mathrm{LHS}})^2}\right) < 0. \tag{D4}$$

The condition in Eq. (D4) holds for the steering inequalities that are defined for qudits, such as proposed in Appendix A and in Refs. [24,41,68].

In our setup, for instance, at fixed loss and noise ($\eta = 0.062$, $p = 0.775$), there are no violations for prime dimensions $d \leq d' = 19$. For prime dimensions $d > 19$,

violation does occur. This provides a nontrivial dependence of total measurement time T on dimension d as in Eq. (C8). Furthermore, a finite dimension which minimizes T requires that it is nonmonotonic on $d > d'$. This is ensured if the above conditions hold and $\lim_{d\to\infty} T = \infty$ [as is the case for Eq. (C8), where at $\lim_{d\to\infty} T = d^4$]. Note that each inequality has to be analyzed case by case. Extending these techniques to suit all families of steering inequalities would be an interesting direction for future work.

[1] Nicolas Gisin and Rob Thew, *Quantum Communication*, Nat. Photonics, **1**, 165 (2007).

[2] Eleni Diamanti, Hoi-Kwong Lo, Bing Qi, and Zhiliang Yuan, *Practical Challenges in Quantum Key Distribution*, npj Quantum Inf. **2**, 16025 (2016).

[3] Mario Krenn, Mehul Malik, Thomas Scheidl, Rupert Ursin, and Anton Zeilinger, *Quantum Communication with Photons* (Springer International Publishing, Cham, 2016), pp. 455–482.

[4] Feihu Xu, Xiongfeng Ma, Qiang Zhang, Hoi-Kwong Lo, and Jian-Wei Pan, *Secure Quantum Key Distribution with Realistic Devices*, Rev. Mod. Phys. **92**, 025002 (2020).

[5] Valerio Scarani, H. Bechmann-Pasquinucci, N. J. Cerf, M. Dusek, N. Lutkenhaus, and M. Peev, *The Security of Practical Quantum Key Distribution*, Rev. Mod. Phys. **81**, 1301 (2009).

[6] Antonio Acín, Nicolas Brunner, Nicolas Gisin, Serge Massar, Stefano Pironio, and Valerio Scarani, *Device-Independent Security of Quantum Cryptography against Collective Attacks*, Phys. Rev. Lett. **98**, 230501 (2007).

[7] Marissa Giustina *et al.*, *Significant-Loophole-Free Test of Bell's Theorem with Entangled Photons*, Phys. Rev. Lett. **115**, 250401 (2015).

[8] Lynden K. Shalm *et al.*, *Strong Loophole-Free Test of Local Realism*, Phys. Rev. Lett. **115**, 250402 (2015).

[9] B. Hensen *et al.*, *Loophole-Free Bell Inequality Violation Using Electron Spins Separated by 1.3 Kilometres*, Nature (London) **526**, 682 (2015).

[10] Philip M. Pearle, *Hidden-Variable Example Based upon Data Rejection*, Phys. Rev. D **2**, 1418 (1970).

[11] N. Gisin and B. Gisin, *A Local Hidden Variable Model of Quantum Correlation Exploiting the Detection Loophole*, Phys. Lett. A **260**, 323 (1999).

[12] H. M. Wiseman, S. J. Jones, and A. C. Doherty, *Steering, Entanglement, Nonlocality, and the Einstein-Podolsky-Rosen Paradox*, Phys. Rev. Lett. **98**, 140402 (2007).

[13] Daniel Cavalcanti and Paul Skrzypczyk, *Quantum Steering: A Review with Focus on Semidefinite Programming*, Rep. Prog. Phys. **80**, 024001 (2017).

[14] Roope Uola, Ana C. S. Costa, H. Chau Nguyen, and Otfried Gühne, *Quantum Steering*, Rev. Mod. Phys. **92**, 015001 (2020).

[15] E. G. Cavalcanti, S. J. Jones, H. M. Wiseman, and M. D. Reid, *Experimental Criteria for Steering and the Einstein-Podolsky-Rosen Paradox*, Phys. Rev. A **80**, 032112 (2009).

[16] D. J. Saunders, S. J. Jones, H. M. Wiseman, and G. J. Pryde, *Experimental EPR-Steering Using Bell-Local States*, Nat. Phys. **6**, 845 (2010).

[17] Bernhard Wittmann, Sven Ramelow, Fabian Steinlechner, Nathan K Langford, Nicolas Brunner, Howard M Wiseman, Rupert Ursin, and Anton Zeilinger, *Loophole-Free Einstein-Podolsky-Rosen Experiment via Quantum Steering*, New J. Phys. **14**, 053030 (2012).

[18] A. J. Bennet, D. A. Evans, D. J. Saunders, C. Branciard, E. G. Cavalcanti, H. M. Wiseman, and G. J. Pryde, *Arbitrarily Loss-Tolerant Einstein-Podolsky-Rosen Steering Allowing a Demonstration over 1 km of Optical Fiber with No Detection Loophole*, Phys. Rev. X **2**, 031003 (2012).

[19] Devin H. Smith *et al.*, *Conclusive Quantum Steering with Superconducting Transition-Edge Sensors*, Nat. Commun. **3**, 625 (2012).

[20] Morgan M. Weston, Sergei Slussarenko, Helen M. Chrzanowski, Sabine Wollmann, Lynden K. Shalm, Varun B. Verma, Michael S. Allman, Sae Woo Nam, and Geoff J. Pryde, *Heralded Quantum Steering over a High-Loss Channel*, Sci. Adv. **4**, e1701230 (2018).

[21] Daniele Cozzolino, Beatrice Da Lio, Davide Bacco, and Leif Katsuo Oxenløwe, *High-Dimensional Quantum Communication: Benefits, Progress, and Future Challenges*, Adv. Quantum Technol. **2**, 1900038 (2019).

[22] Manuel Erhard, Mario Krenn, and Anton Zeilinger, *Advances in High Dimensional Quantum Entanglement*, Nat. Rev. Phys. **2**, 365 (2020).

[23] Nicolas Brunner, S. Pironio, A. Acin, N. Gisin, A. A. Methot, and V. Scarani, *Testing the Dimension of Hilbert Spaces*, Phys. Rev. Lett. **100**, 210503 (2008).

[24] Sébastien Designolle, *Robust Genuine High-Dimensional Steering with Many Measurements*, Phys. Rev. A **105**, 032430 (2022).

[25] Tamás Vertesi, Stefano Pironio, and Nicolas Brunner, *Closing the Detection Loophole in Bell Experiments Using Qudits*, Phys. Rev. Lett. **104**, 060401 (2010).

[26] H. Bechmann-Pasquinucci and W. Tittel, *Quantum Cryptography Using Larger Alphabets*, Phys. Rev. A **61**, 062308 (2000).

[27] Nicolas J. Cerf, Mohamed Bourennane, Anders Karlsson, and Nicolas Gisin, *Security of Quantum Key Distribution Using d-Level Systems*, Phys. Rev. Lett. **88**, 127902 (2002).

[28] Mehul Malik and Robert W Boyd, *Quantum Imaging Technologies*, Nuovo Cimento **37**, 273 (2014).

[29] Lana Sheridan and Valerio Scarani, *Security Proof for Quantum Key Distribution Using Qudit Systems*, Phys. Rev. A **82**, 030301(R) (2010).

[30] J. Nunn, L. J. Wright, C. Söller, L. Zhang, I. A. Walmsley, and B. J. Smith, *Large-Alphabet Time-Frequency Entangled Quantum Key Distribution by Means of Time-to-Frequency Conversion*, Opt. Express **21**, 15959 (2013).

[31] Zheshen Zhang, Jacob Mower, Dirk Englund, Franco N. C. Wong, and Jeffrey H. Shapiro, *Unconditional Security of Time-Energy Entanglement Quantum Key Distribution Using Dual-Basis Interferometry*, Phys. Rev. Lett. **112**, 120506 (2014).

[32] Mohammad Mirhosseini, Omar S Magaña-Loaiza, Malcolm N O'Sullivan, Brandon Rodenburg, Mehul Malik, Martin P J Lavery, Miles J Padgett, Daniel J Gauthier, and Robert

W Boyd, *High-Dimensional Quantum Cryptography with Twisted Light*, New J. Phys. **17**, 033033 (2015).
[33] Matej Pivoluska, Marcus Huber, and Mehul Malik, *Layered Quantum Key Distribution*, Phys. Rev. A **97**, 032312 (2018).
[34] Sebastian Ecker *et al.*, *Overcoming Noise in Entanglement Distribution*, Phys. Rev. X **9**, 041042 (2019).
[35] F. Zhu, M. Tyler, N. H. Valencia, M. Malik, and J. Leach, *Is High-Dimensional Photonic Entanglement Robust to Noise?*, AVS Quantum Sci. **3**, 011401 (2021).
[36] Natalia Herrera Valencia, Suraj Goel, Will McCutcheon, Hugo Defienne, and Mehul Malik, *Unscrambling Entanglement through a Complex Medium*, Nat. Phys. **16**, 1112 (2020).
[37] Huan Cao *et al.*, *Distribution of High-Dimensional Orbital Angular Momentum Entanglement over a 1 km Few-Mode Fiber*, Optica **7**, 232 (2020).
[38] Manuel Erhard, Mehul Malik, and Anton Zeilinger, *A Quantum Router for High-Dimensional Entanglement*, Quantum Sci. Technol. **2**, 014001 (2017).
[39] Fabian Steinlechner, Sebastian Ecker, Matthias Fink, Bo Liu, Jessica Bavaresco, Marcus Huber, Thomas Scheidl, and Rupert Ursin, *Distribution of High-Dimensional Entanglement via an Intra-City Free-Space Link*, Nat. Commun. **8**, 15971 (2017).
[40] Mhlambululi Mafu, Angela Dudley, Sandeep Goyal, Daniel Giovannini, Melanie McLaren, Miles J. Padgett, Thomas Konrad, Francesco Petruccione, Norbert Lütkenhaus, and Andrew Forbes, *Higher-Dimensional Orbital-Angular-Momentum-Based Quantum Key Distribution with Mutually Unbiased Bases*, Phys. Rev. A **88**, 032305 (2013).
[41] Sébastien Designolle, V. Srivastav, R. Uola, N. H. Valencia, W. McCutcheon, M. Malik, and N. Brunner, *Genuine High-Dimensional Quantum Steering*, Phys. Rev. Lett. **126**, 200404 (2021).
[42] Rui Qu, Y. Wang, M. An, F. Wang, Q. Quan, H. Li, H. Gao, F. Li, and P. Zhang, *Retrieving High-Dimensional Quantum Steering from a Noisy Environment with N Measurement Settings*, Phys. Rev. Lett. **128**, 240402 (2022).
[43] Marcus Huber and Marcin Pawłowski, *Weak Randomness in Device-Independent Quantum Key Distribution and the Advantage of Using High-Dimensional Entanglement*, Phys. Rev. A **88**, 032309 (2013).
[44] Takuya Ikuta and Hiroki Takesue, *Implementation of Quantum State Tomography for Time-Bin Qudits*, New J. Phys. **19**, 013039 (2017).
[45] Nicolas K. Fontaine, Roland Ryf, Haoshuo Chen, David T. Neilson, Kwangwoong Kim, and Joel Carpenter, *Laguerre-Gaussian Mode Sorter*, Nat. Commun. **10**, 1865 (2019).
[46] Suraj Goel *et al.*, Inverse-Design of High-Dimensional Quantum Optical Circuits in a Complex Medium, arXiv:2204.00578.
[47] William K. Wootters and Brian D. Fields, *Optimal State-Determination by Mutually Unbiased Measurements*, Ann. Phys. (N.Y.) **191**, 363 (1989).
[48] Ana Belén Sainz, Yelena Guryanova, Will McCutcheon, and Paul Skrzypczyk, *Adjusting Inequalities for Detection-Loophole-Free Steering Experiments*, Phys. Rev. A **94**, 032122 (2016).
[49] This assumes a fiber loss of 0.18 to 0.2 dB/km, as provided by ultralow-loss telecom fiber.
[50] Frédéric Bouchard, Natalia Herrera Valencia, Florian Brandt, Robert Fickler, Marcus Huber, and Mehul Malik, *Measuring Azimuthal and Radial Modes of Photons*, Opt. Express **26**, 31925 (2018).
[51] Hammam Qassim, Filippo M. Miatto, Juan P. Torres, Miles J. Padgett, Ebrahim Karimi, and Robert W. Boyd, *Limitations to the Determination of a Laguerre-Gauss Spectrum via Projective, Phase-Flattening Measurement*, J. Opt. Soc. Am. B **31**, A20 (2014).
[52] Serge Massar and Stefano Pironio, *Violation of Local Realism versus Detection Efficiency*, Phys. Rev. A **68**, 062109 (2003).
[53] Reinhard F. Werner, *Quantum States with Einstein-Podolsky-Rosen Correlations Admitting a Hidden-Variable Model*, Phys. Rev. A **40**, 4277 (1989).
[54] Vatshal Srivastav, Natalia Herrera Valencia, Saroch Leedumrongwatthanakun, Will McCutcheon, and Mehul Malik, *Characterising and Tailoring Spatial Correlations in Multimode Parametric Down-Conversion*, Phys. Rev. Appl. **18**, 054006 (2022).
[55] Natalia Herrera Valencia, Vatshal Srivastav, Matej Pivoluska, Marcus Huber, Nicolai Friis, Will McCutcheon, and Mehul Malik, *High-Dimensional Pixel Entanglement: Efficient Generation and Certification*, Quantum **4**, 376 (2020).
[56] Victor Arrizón, Ulises Ruiz, Rosibel Carrada, and Luis A. González, *Pixelated Phase Computer Holograms for the Accurate Encoding of Scalar Complex Fields*, J. Opt. Soc. Am. A **24**, 3500 (2007).
[57] Mohammad Mirhosseini, Omar S. Magaña-Loaiza, Changchen Chen, Brandon Rodenburg, Mehul Malik, and Robert W. Boyd, *Rapid Generation of Light Beams Carrying Orbital Angular Momentum*, Opt. Express **21**, 30196 (2013).
[58] Michael Kues, Christian Reimer, Joseph M. Lukens, William J. Munro, Andrew M. Weiner, David J. Moss, and Roberto Morandotti, *Quantum Optical Microcombs*, Nat. Photonics **13**, 170 (2019).
[59] Daniel Llewellyn *et al.*, *Chip-to-Chip Quantum Teleportation and Multi-Photon Entanglement in Silicon*, Nat. Phys. **16**, 148 (2020).
[60] Bo Jing *et al.*, *Entanglement of Three Quantum Memories via Interference of Three Single Photons*, Nat. Photonics **13**, 210 (2019).
[61] M. Pompili *et al.*, *Realization of a Multinode Quantum Network of Remote Solid-State Qubits*, Science **372**, 259 (2021).
[62] Antonio Acín, Daniel Cavalcanti, Elsa Passaro, Stefano Pironio, and Paul Skrzypczyk, *Necessary Detection Efficiencies for Secure Quantum Key Distribution and Bound Randomness*, Phys. Rev. A **93**, 012319 (2016).
[63] Cyril Branciard, Eric G. Cavalcanti, Stephen P. Walborn, Valerio Scarani, and Howard M. Wiseman, *One-Sided Device-Independent Quantum Key Distribution: Security, Feasibility, and the Connection with Steering*, Phys. Rev. A **85**, 010301(R) (2012).
[64] Joseph F. Fitzsimons, *Private Quantum Computation: An Introduction to Blind Quantum Computing and Related Protocols*, npj Quantum Inf. **3**, 23 (2017).

[65] Fuad Kittaneh, *Norm Inequalities for Certain Operator Sums*, J. Funct. Anal. **143**, 337 (1997).

[66] Marco Tomamichel, Serge Fehr, Jędrzej Kaniewski, and Stephanie Wehner, *A Monogamy-of-Entanglement Game with Applications to Device-Independent Quantum Cryptography*, New J. Phys. **15**, 103002 (2013).

[67] Paul Skrzypczyk and Daniel Cavalcanti, *Loss-Tolerant Einstein-Podolsky-Rosen Steering for Arbitrary-Dimensional States: Joint Measurability and Unbounded Violations under Losses*, Phys. Rev. A **92**, 022354 (2015).

[68] Paul Skrzypczyk and Daniel Cavalcanti, *Maximal Randomness Generation from Steering Inequality Violations Using Qudits*, Phys. Rev. Lett. **120**, 260401 (2018).